

TOPSIS vs Quality Loss Function Multi-Criteria Optimization of Mechanical Performance in Laser Spot Welding Process

Ruba Khalil *, Bassim Bachy 

Department of Mechanical Engineering, College of Engineering, University of Baghdad, Baghdad, Iraq

ABSTRACT

When selecting a material for product design, the focus is on its mechanical properties, a standard requirement in most applications. This paper's research aimed to determine if better calibration of polymethyl methacrylate (PMMA) material samples welded with laser spot welding could be achieved by verifying joint strength performance and modulus of elasticity. Tensile tests were conducted using a universal testing machine with a 100 kN load capacity. Parameters studied included laser power, welding velocity, laser focus diameter, and spot geometric size. An orthogonal L9 array with three levels was used. Multi-objective optimization techniques TOPSIS-Quality Loss Function were used, and the results were compared. It was discovered that the first experiment among the nine experiments had the best multi-quality features with the following parameters: laser power of 10 W, welding velocity of 10 mm/s, laser focus diameter of 0.002 mm, and spot geometric size of 4 mm. It was observed that the geometric spot design is the most effective parameter for quality at a small size. It was proven that the smaller size of the geometric spot increases the strength and stiffness of the welded product.

Keywords: Laser spot welding process, Mechanical properties, Tensile test, Joint strength, Modulus of elasticity, PMMA material.

1. INTRODUCTION

Polymeric materials are lightweight, strong, inexpensive, easy to make, versatile, recyclable, and corrosion-resistant. Making them suitable for various, like aeroplane design, shipbuilding, automobiles, and building materials, and in the medical field, which has driven the need to enhance their functionality, reliability, longevity, and cost-effectiveness, expanding their uses (Haqi and Olfat, 2021; Alasfar et al., 2022; Anwera and Acherjee, 2024; Kucukoglu et al., 2023). Manufacturing complicated polymer items in one piece is not always possible, practicable, or economical. To solve this problem, several polymer joining techniques have been developed; introduced in the 1980s, the laser transmission welding LTW is a relatively new addition to the extensive array of polymer joining

*Corresponding author

Peer review under the responsibility of University of Baghdad.

<https://doi.org/10.31026/j.eng.2025.07.02>



This is an open access article under the CC BY 4 license (<http://creativecommons.org/licenses/by/4.0/>).

Article received: 23/01/2025

Article revised: 16/03/2025

Article accepted: 27/03/2025

Article published: 01/07/2025



techniques; but it gained popularity in the late 1990s and early 2000s (Acherjee, 2020). After more than ten years of research, laser welding is a well-established technique that threatens older methods like adhesive bonding or ultrasonic welding (Olowinsky and Roesner, 2012). Polymethyl methacrylate, or PMMA, is a transparent thermoplastic polymer that transmits 92% of light; because of its transparency, formability, recyclability, machinability, and affordability, it is increasingly utilized in construction, agriculture, aviation, optical instruments, and lighting (Huang et al., 2021). PMMA possesses exceptional qualities such as its processing ability, high tensile strength, and transparency (Forte et al., 2021). A quick, accurate, and high-altitude method for joining thin plates, laser spot welding is used in various sectors, including electronics, automotive, and aerospace. Fast welding, accurate outcomes, high energy density, and environmentally beneficial properties are some of its features (Li et al., 2021).

Laser parameters have been improved via evaluations using various techniques, including restricted factor analysis, Design of Experiments DOE, and synthetic intellect because it is possible to analyze the effects of several input parameters on a desired result. DOE is frequently used for experiment design (Kucukoglu et al., 2023). Furthermore, much research has been done utilizing lasers, emphasizing choosing the best parameters and designing experiments. Literature examples; choosing the best parameters include the experimental design by Taguchi and ANOVA methods of laser engraving (Imran et al., 2021); The study of laser cutting that developed an experiment-based tool using the central composite design and response surface methodology (Hassan and Bachy, 2023). The experimental design of laser direct structuring (Bachy et al., 2018; Bachy and Franke, 2015); And the experimental design of laser welding (Dave et al., 2022; Ilie et al., 2020). Technique for Order Preference by Similarity to Ideal Solution TOPSIS is a method for evaluating multiple criteria; it was created by Hwang and Yoon in 1981 and later improved by Yoon in 1987 and Hwang, Lai, and Liu in 1993. TOPSIS is based on choosing an option closest to the positive ideal solution and farthest from the negative ideal solution (Kanaujia et al., 2022). The following phases describe Taguchi's Quality Loss Function (QLF) quality engineering approach: there is an ideal target value for every engineering output; any departure from the goal results in a loss; these losses include decreased life and deteriorated performance; the output response deviates more from the objective as loss increases; reducing the departure of performance measures from the target is the aim of Robust Design (RD) (Tshibangu, 2018).

High-strain deformation causes materials to change shape permanently, known as plastic deformation, which can lead to failure. The polymer behaves like a linear elastic solid at low loads and strains. The proportional limit is where the behavior starts to become non-linear, the yield point marks the start of permanent deformation on the stress-strain curve, and yield strength and elongation at yield refer to the stress and elongation at this point. Beyond the yield point, the material enters the plastic region, leading to breakage from further elongation and strain hardening, described by ultimate strength and elongation at break (Milisavljevic et al., 2012). So, failure can be avoided by tracking its modulus and forecasting the polymer component's lifespan (Judawisastra et al., 2019).

In the field of laser welding for polymers, many studies have focused on investigating the strength of the weld joint. Depending on the combination of process conditions, the various temperature fields inside the seam regulate the weld seam's strength. As a result, the ideal weld quality may be achieved under ideal process circumstances (Kumar Goyal et al., 2023). (Acherjee, 2020) focused on welding acrylic to acrylonitrile butadiene styrene via



laser transmission. Up until a certain point, welding speed and stand-off distance improve weld strength; after that, they decrease, and weld strength is significantly impacted by stand-off distance, which is followed by laser power, welding speed, and clamp pressure.

(Rudrapati et al., 2019) investigated the effects of process variables on the strength of the weld joints while laser welding acrylic plastic. Joint strength is most significantly impacted by clamping pressure, which is followed by stand-off distance and current. The Taguchi approach yielded ideal welding parameters: a pressure of 10 bar, a stand-off distance of 34 mm, and a current of 32 A. The validity of the Taguchi optimization process is supported by a confirmation test, which verifies the increased weld joint strength.

(Girish Kumar et al., 2023) focused on laser transmission welding (LTW) of two 3D-printed polylactic acid sheets in a lap welding setup. Analysis of variance (ANOVA) showed that scanning speed significantly affected tensile strength, contributing 95.63% to the maximum weld strength. The Grey-Taguchi method identified optimal conditions for joint strength as a power of 20 W, speed of 5 mm/s, and spot size of 250 mm.

(Shaker et al., 2020) the Taguchi method was used to find the best process parameters for PMMA laser transmission welding. The best welding parameters for maximum strength are a speed of 15 mm/s, a spot size of 2.5 mm, and a power of 10 W.

(Girish Kumar et al., 2021) studied two polyamide plastic plates welded using laser transmission welding. ANOVA analysis indicated that scanning speed and power affected weld shear strength, contributing 38.53% and 28.7%, respectively. The optimal conditions for maximum joint strength from the Grey-Taguchi method were identified as P3 SS2 NOP1, Power of 220 W, scanning speed of 195 mm/s, and two passes.

This study optimized the laser transmission spot welding process parameters on the mechanical properties represented by the joint strength and the modulus of elasticity of the welded joint to PMMA pieces with the same thicknesses. The Analysis of Variance (ANOVA) of the Regression (REG) model enhanced individual objectives. Multi-objective optimization techniques were used, as Taguchi Quality Loss Function, and the result was confirmed and compared using the TOPSIS method, selected criteria that matched all responses. A fiber laser was used with a wavelength of 1064 nm. A fiber laser was used with a wavelength of 1064 nm.

2. EXPERIMENTAL WORK

As seen in **Fig. 1 (a)**, the transparent and absorptive polymethylmethacrylate or PMMA samples were shaped into rectangular forms measuring 80 mm by 40 mm and having a thickness of 2.4 mm. A laser system with a wavelength of 1064 nm, a maximum laser power of 50 W, a maximum pulse frequency of 200 kHz, a maximum laser pulse duration of 20 nanoseconds, a total beam diameter of 30 μm , and a top scanning speed of 10,000 mm/s was used in several tests. The chosen welding parameters and their limitations, units, and symbols are shown in **Table 1**. These numbers were released after several previous tests and laboratory studies .

The experiment and the number of replications related to the process parameters were designed using the Taguchi L9 orthogonal array from the Minitab 21 program, as shown in **Table 2**. EzCad 2 CAD/CAM software has been employed to set up and develop parameters to generate the CAD design of the recommended welding strategy (welding profile). The plate samples were set up and supported during welding using a mold made of PMMA polymer with a thickness of 10 mm, as shown in **Fig. 1 (b)**. It has been divided in half and fastened to the machine's base using the appropriate screws and bolts. A groove in this mold

holds the sample in place during welding, and the applied pressure is measured using a load cell positioned underneath the sample. An LCD installed in the appropriate box for this setup shows the outcome of the spread and uniform pressure, as shown in **Fig. 1 (c)**. Clamp pressure improves thermal conduction at the contact area. This enhances heat transfer from the bottom polymer to the top polymer, improving melt flow in the weld pool, essential for mixing and cross-linking the polymer chains that form the weld (**Acherjee, 2021**).

Table 1. Process control parameters and their boundaries

| Symbol | Parameters with their Unit | Levels | | |
|--------|----------------------------|---------|---------|---------|
| | | Level 1 | Level 2 | Level 3 |
| A | Laser Power (W) | 10 | 20 | 30 |
| B | Welding Velocity (mm/s) | 10 | 15 | 20 |
| C | Laser Focus Diameter (mm) | 0.002 | 0.004 | 0.006 |
| D | Spot Geometric Size (mm) | 4 | 6 | 8 |

Table 2. The experimental design of process parameters

| Exp. no. | Input Parameters | | | |
|----------|------------------|---------|--------|--------|
| | A (W) | B (m/s) | C (mm) | D (mm) |
| 1 | 10 | 10 | 0.002 | 4 |
| 2 | 10 | 15 | 0.004 | 6 |
| 3 | 10 | 20 | 0.006 | 8 |
| 4 | 20 | 10 | 0.004 | 8 |
| 5 | 20 | 15 | 0.006 | 4 |
| 6 | 20 | 20 | 0.002 | 6 |
| 7 | 30 | 10 | 0.006 | 6 |
| 8 | 30 | 15 | 0.002 | 8 |
| 9 | 30 | 20 | 0.004 | 4 |

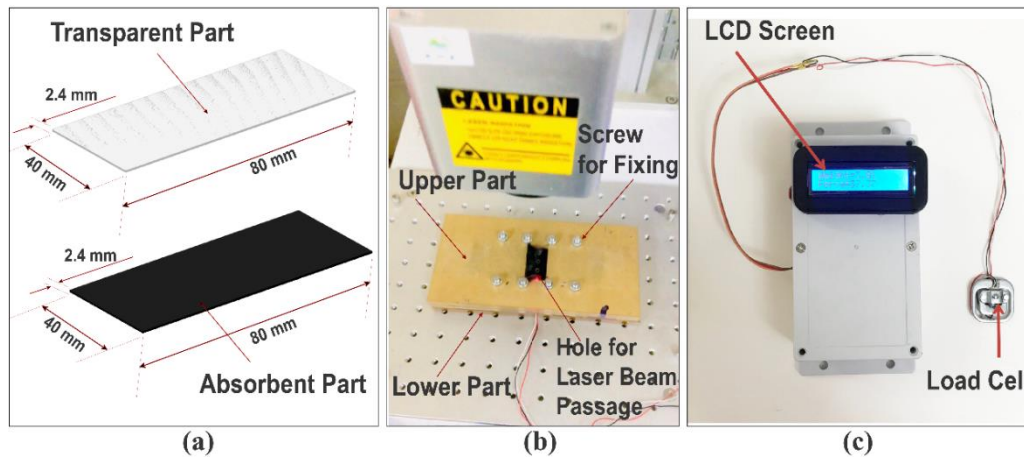


Figure 1. (a) Test specimen, (b) Mold for welding process, and (c) Pressure measuring device containing LCD screen.

A universal testing machine was utilized to perform the tensile test to find out the mechanical properties of the welded specimens, such as joint strength and modulus of elasticity, with the model WDW-100, maximum load capacity of 100 kN, and power supply 1-phase, 220 V, 50 Hz/60 Hz, the machine has a computer control electronic universal gives

computerized output data as shown in Fig. 2 (a), uniaxial tension experiments were performed on specimens using a screw-driven load frame, The specimens are mounted by their ends into the holding grips of the testing apertures, under a constant speed of 0.5 mm/min at room temperature in order to prevent misalignment, limit welding moment in the weld seam during the lap shear test, and maintain consistent lapping for each run. A fixture plate held a welding specimen. It measured 20 mm by 40 and was posted with each sample for several runs, as shown in Fig. 2 (b). The tensile test begins slowly and continues until the weld sample breaks.

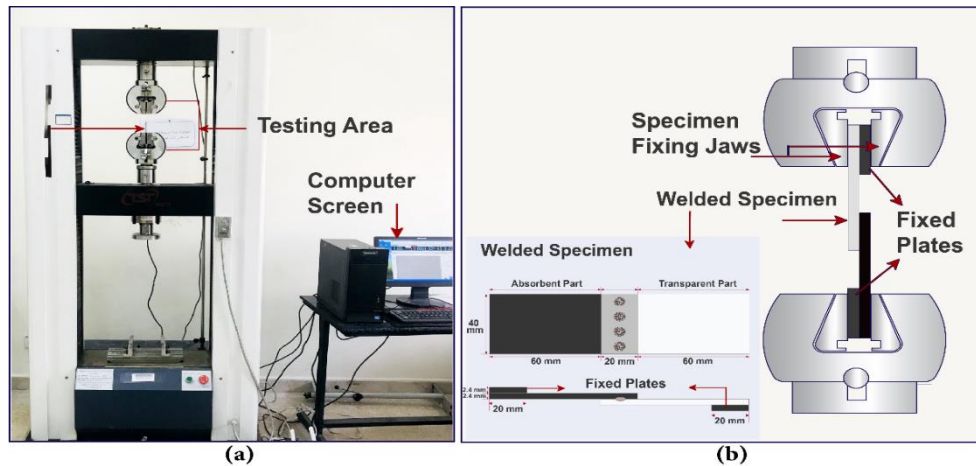


Figure 2. (a) A universal testing machine has a computer control, and (b) The testing area contains a screw-driven load frame and test specimen.

3. DEVELOPMENT OF MATHEMATICAL MODELS

In order to help create the model in use, the optimization must consider system parameters or model variables that represent laser power, welding velocity, laser focus diameter, and spot geometric size. In order to assess the quality of the welding, objective functions or criteria for optimization must be established that can serve as a guide. These criteria include the joint strength and modulus of elasticity. An accurate and functional model that describes the system can be used to predict how the system will respond to parameters or inputs. This experiment uses the TOPSIS-Quality Loss Function (QLF) for optimizations. A single-objective optimization by a regression analysis was conducted to understand how input factors affect output variables. The model used Minitab 21 software. A regression equation was created to predict the output variables, helping to develop a mathematical model for the laser spot welding process as Eq. (1).

$$\hat{y} = \beta_0 + \beta_1 x_1 + \beta_2 x_2 + \dots + \beta_k x_k \tag{1}$$

Where: B_0 , B_1 , and B_2 are the constants, and Y represents the dependent or response variables.

3.1 Taguchi Quality Loss Function Approach

Taguchi's quality loss function is an engineering quality system that uses effective strategies rather than complex statistical methods. It significantly enhances product and process quality. Taguchi argues that any deviation from the target value is a loss, even within



acceptable limits. It emphasizes achieving goals accurately to avoid losses, as nearing boundaries results in double the loss. This approach prioritizes quality throughout the engineering process and aims to minimize losses and optimize quality outcomes for products and processes (Khalaf and Kadhim, 2020).

Quality characteristics can be classified into higher-is-better, lower-is-better, or nominal-is-best. In this case of the study, there is no need for lower-is-better. The procedures include the steps below (Rane et al., 2011).

Step1: Higher-is-better H_i , as Eq. (2).

$$H_i = \frac{1}{z} \sum_{Z=1}^n \frac{1}{y_{iz}^2} \quad (2)$$

Where:

y_{iz} is the experimental outcome of (i) for every experimental run, and z is the number of tests that were repeated in that run.

Step2: Loss functions are normalized L_{ij} based on their maximum value due to different engineering units. Nominal-is-best as Eq. (3).

$$L_{ij} = \frac{H_{ij}}{M_{i*}} \quad (3)$$

Where:

M_{i*} is the highest quality loss for the (i) quality feature in all test settings and j is the experiment condition.

Step3: The total normalized loss is obtained by integrating the several normalized loss functions using a weighted (W_i) approach for the (i) objectives. Eq. (4) provides the formula for the total loss function (TQ_j) in the (j) experiment condition, and (n) is the quantity of response attributes denoted.

$$TQ_j = \sum_{i=1}^n W_i L_{ij} \quad (4)$$

Different responses' importance on welding quality was evaluated, and specific weights were given based on their significance, totalling 1. The joint strength, measuring the maximum strength welded samples can withstand, had the highest weight of 0.60. The modulus of elasticity was assigned a weight of 0.40.

Step4: Next, the multi-response signal-to-noise ratio (SNR_j) for the (j) experiment condition, the total normalized loss is obtained by using the calculation for the S/N ratio Eq. (5).

$$SNR_j = -10 \log_{10} (TQ_j) \quad (5)$$

3.2 TOPSIS Approach

Hwang and Yoon, in 1981 created the (TOPSIS), a multi-criteria decision analysis (MCDA) technique. The fundamental principle at the earlier stage was that the option selected indicates the geometrical distance that is the least from the positive ideal solution and the longest from the negative ideal solution. This method chooses the best option, which is the one that is closest to the positive ideal solution and the one that is far from the negative ideal solution. Using the proper algorithm, TOPSIS may be seen as a practical decision-making method since it makes trade-offs between the criteria, with a poor outcome in one criterion



being offset by a better result in another (Sultana and Dhar, 2021). The procedures include the steps below (Sharma et al., 2022; Chokkalingam et al., 2022; Umamaheswarrao, 2023; Van Pham, 2023).

Step 1: The qualities have been identified, and the options have been decided. Two qualities have been taken into consideration for the evaluation of the nine choices in this issue. Joint strength and modulus of elasticity are regarded as advantageous characteristics and should be maximized (higher the better).

Step 2: designed a decision matrix $(R_{ij})_{m \times r}$ consisting of 'm (9)' attributes 'r (2)' alternatives.

Step 3: Development of the normalized decision matrix (R_{ij}) removes units from all output objectives. Investigated attributes are normalized using Eq. (6). Where, $i =$ trial 1 to 9; $j =$ objective 1, and 2

$$N_{ij} = \frac{R_{ij}}{\sqrt{\sum_{i=1}^j R_{ij}^2}} \tag{6}$$

Step 4: The weighted decision normalized matrix is obtained. (W_j) represent each attribute's weight. the weighted decision normalized matrix (Q_{ij}) , is calculated as Eq. (7)

$$Q_{ij} = N_{ij} \times W_j \tag{7}$$

The target weights were set by importance, totalling summation one. Joint strength received 0. 60, and modulus of elasticity 0. 40.

Step 5: Find the answers for the positive ideal (Q^+) and negative ideals (Q^-) .

$$Q^+ = (Q_1^+, Q_2^+, Q_3^+, Q_4^+ \dots \dots \dots Q_n^+) \text{Where, } Q_j^+ = \max \text{ or } \min Q_{ij}^+ \tag{8}$$

$$Q^- = (Q_1^-, Q_2^-, Q_3^-, Q_4^- \dots \dots \dots Q_n^-) \text{Where, } Q_j^- = \max \text{ or } \min Q_{ij}^- \tag{9}$$

Step 6: Finding the alternate measures of separation from ideal, positive S_i^+ and negative S_i^- .as Eq. (10 and 11).

$$S_i^+ = \sqrt{\sum (Q_{ij} - Q_j^+)^2} \quad i = 1,2,\dots,m \tag{10}$$

$$S_i^- = \sqrt{\sum (Q_{ij} - Q_j^-)^2} \quad i = 1,2,\dots,m \tag{11}$$

Step 7: Finding the preferred value (P_i) for the proximity coefficient. The relative distance between a particular alternative and the optimal solution is written as Eq. (12)

$$P_i = \frac{S_i^-}{(S_i^+ - S_i^-)} \tag{12}$$

4. RESULTS AND DISCUSSION

4.1 Experimental Results

The joint strength and modulus of elasticity were calculated using the equations using tensile test data and curves. The tensile strength is calculated by dividing the greatest force attained during the Pmax test by the area (Dowling, 2013).

$$\sigma (N/mm^2) = P_{max}/A_i \tag{13}$$



where: σ : the joint strength (N/mm²), Pmax: max load (N) for each experiment, and Ai: The area affected by welding (mm²).

The ultimate load was determined from tensile tests and was divided by the welding area. Nine experiments were categorized into three weld regions based on spot dimensions. The weld zone areas were calculated as follows: 50.24 mm² for a 4 mm spot, 113.04 mm² for a 6 mm spot and 200.96 mm² for an 8 mm spot. The modulus of elasticity (E) was calculated using Hooke's Law, where E (N/mm²)= Stress/Strain. By determining a straight line for elastic deformation, the elastic modulus (Young's modulus) can be found by analyzing stresses and strains at two points. Laboratory data collected digitally can be used to find the slope for E using the equation (Dowling, 2013; AlMaadeed et al.,2020).

$$E = \frac{\sigma_B - \sigma_A}{\epsilon_B - \epsilon_A} \tag{14}$$

Fig. 3 shows the stress-strain curve of one sample and the slope used to calculate the modulus of elasticity along the straight line. Table 3 displays the experimental setup, including the Taguchi approach's estimation of process parameters and responses for modulus of elasticity and joint strength. The ultimate tensile strength was lower than the base material; Thus, it is possible for laser-welded joints to be weaker than their base materials (Rudrapati et al., 2019). In primarily due to the heat input, minimal thermal distortion, and surrounding heat-affected zone HAZ (Hussein and Bachy, 2024; Jiang et al., 2015; Farabi et al., 2012). Moreover, such a process doesn't need joint strength higher than that for base materials.

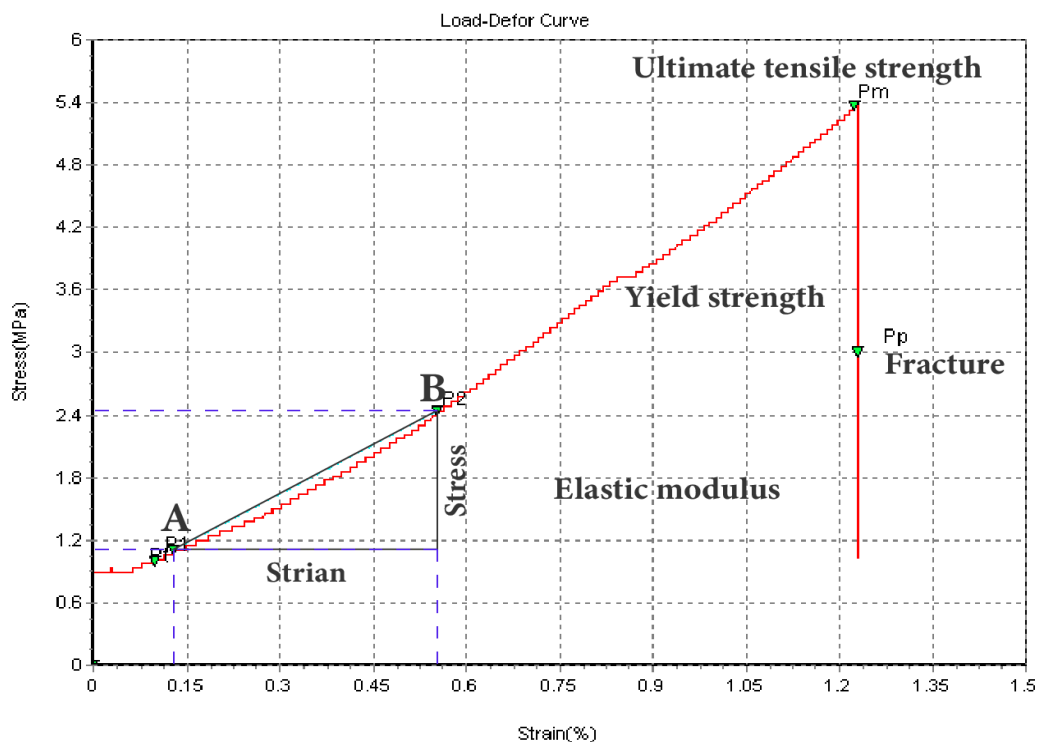


Figure 3. The stress-strain curve from a tensile test shows the slope for calculating the modulus of elasticity.



Table 3. Experimental Results

| Exp. no. | Input Parameters | | | | The Objectives | |
|----------|------------------|---------|--------|--------|-------------------------------------|--|
| | A (W) | B (m/s) | C (mm) | D (mm) | Joint Strength (N/mm ²) | Modulus of Elasticity (N/mm ²) |
| 1 | 10 | 10 | 0.002 | 4 | 17.06807325 | 10.31870419 |
| 2 | 10 | 15 | 0.004 | 6 | 6.502123142 | 3.911444278 |
| 3 | 10 | 20 | 0.006 | 8 | 3.147392516 | 1.991664839 |
| 4 | 20 | 10 | 0.004 | 8 | 3.545481688 | 2.17412152 |
| 5 | 20 | 15 | 0.006 | 4 | 16.91878981 | 9.832067282 |
| 6 | 20 | 20 | 0.002 | 6 | 5.130927105 | 3.345903955 |
| 7 | 30 | 10 | 0.006 | 6 | 6.524239207 | 3.837912088 |
| 8 | 30 | 15 | 0.002 | 8 | 3.86892914 | 2.130116959 |
| 9 | 30 | 20 | 0.004 | 4 | 15.17714968 | 10.9279476 |

4.2 Modelling Results

The results of the multiple regression model's Analysis of Variance (ANOVA) are shown in **Table 4**, along with the contribution percentage, F-values, and P-values for joint strength and modulus of elasticity. ANOVA is a frequently used statistical method to evaluate how individual answer changes affect the total variance brought about by component variations (**Sabry et al., 2024**). To determine if a parameter significantly affects the selected welding quality, the F-value, also known as Isher's ratio, is compared with the standard P table value (P 0.05) at a 5% significance level (95% confidence level). The associated variables are considered statistically significant if the P-values in the table are less than 0.05.

Table 4 shows the results in the joint strength, indicating that spot geometric size has the greatest impact, and it is statistically significant with an F-value of 31.37 and a contribution percentage of 87.90%. The remaining three parameters, welding velocity, laser power, and laser focus diameter, did not exhibit statistical significance, with low F-values of 0.29, 0.03, and 0.01, and contribution percentages of 0.80%, 0.08%, and 0.02%, respectively. As for the modulus of elasticity, it was observed that the most significant impact was of the spot geometric size, and they are statistically significant with an F-value of 30.24 and a contribution percentage of 88.26%, followed by a low impact of laser power with an F-value of 0.02 and a contribution percentage of 0.07%, so it is not statistically significant, with zero impact of welding velocity and laser focus diameter, so it is not statistically significant.

Table 4. Contribution percentage, F-values, and P-values according to ANOVA of multiple regression model for objectives

| Parameters | Objectives | | | | | |
|-------------------|-------------------------------------|----------|----------|--|----------|----------|
| | Joint strength (N/mm ²) | | | Modulus of Elasticity (N/mm ²) | | |
| | Contribution% | F-values | P-values | Contribution% | F-values | P-values |
| Regression | 88.79% | 7.92 | 0.035 | 88.33% | 7.57 | 0.038 |
| A | 0.08% | 0.03 | 0.876 | 0.07% | 0.02 | 0.888 |
| B | 0.80% | 0.29 | 0.621 | 0.00% | 0 | 0.989 |
| C | 0.02% | 0.01 | 0.943 | 0.00% | 0 | 0.978 |
| D | 87.90% | 31.37 | 0.005 | 88.26% | 30.24 | 0.005 |

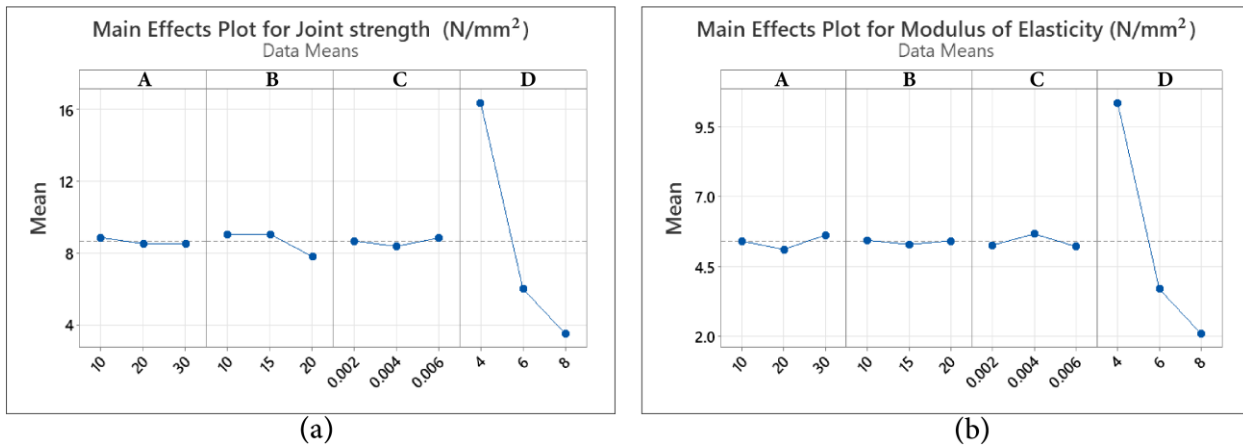


Figure 4. Main effects plot of parameters on objectives for (a) joint strength (N/mm²) and (b) modulus of elasticity (N/mm²).

To confirm the multiple regression analysis, the main effect plot of parameters on joint strength and modulus of elasticity appears in **Fig. 4**, which matches the results. It is identified from the main effect plot from **Fig. 4(a)** that the joint strength increases with the decrease in spot geometric size at 4 mm. This parameter has the largest impact on this objective. In contrast, the other parameters have very little influence. A welding velocity from 10 mm/s to 15 mm/s and laser power at 10 W increased the joint strength, while the laser focus diameter had little to no impact. From **Fig. 4 (b)**, the modulus of elasticity decreases with the increase of spot geometric size from 6 mm to 8 mm and increases at 4 mm. At the same time, the other parameters have very little influence. Laser power has a negative impact between 10 W and 20 W and a positive effect above 20 W to 30 W. In comparison, the laser focus diameter has a positive impact between 0.002 mm and 0.004 mm and a negative effect above 0.004 mm and 0.006 mm. However, the welding velocity has no impact.

The complete mathematical models of the answers related to the model of equation 1 are shown in Eq. (15) through (16). These models may be used for both prediction and optimization within the same design:

$$\text{Joint strength (N/mm}^2\text{)} = 30.00 - 0.019 A - 0.123 B + 44 C - 3.217 D \quad (15)$$

$$\text{Modulus of Elasticity (N/mm}^2\text{)} = 17.63 + 0.0112 A - 0.002 B - 11 C - 2.065 D \quad (16)$$

4.3 Confirmation and Validity of the Model

Prediction accuracy is crucial in practical experiments, as it significantly influences decision-making and the success of any endeavor. Comparing experimental testing and predicted regression results, data was approaching at an acceptable rate between experimental and predicted values for both joint strength and modulus of elasticity, as shown in **Fig. 5 (a) and (b)**. Predictive optimization technology provides trends of errors in prediction results and automatically reflects them to optimization. The average error value in joint strength is 29.45%. In comparison, the average error value in modulus of elasticity is 31.54%, as shown in **Fig. 6**. These models can be used for analysis and optimization as the observed errors are approaching an acceptable rate within the typical error range of the modeling tool

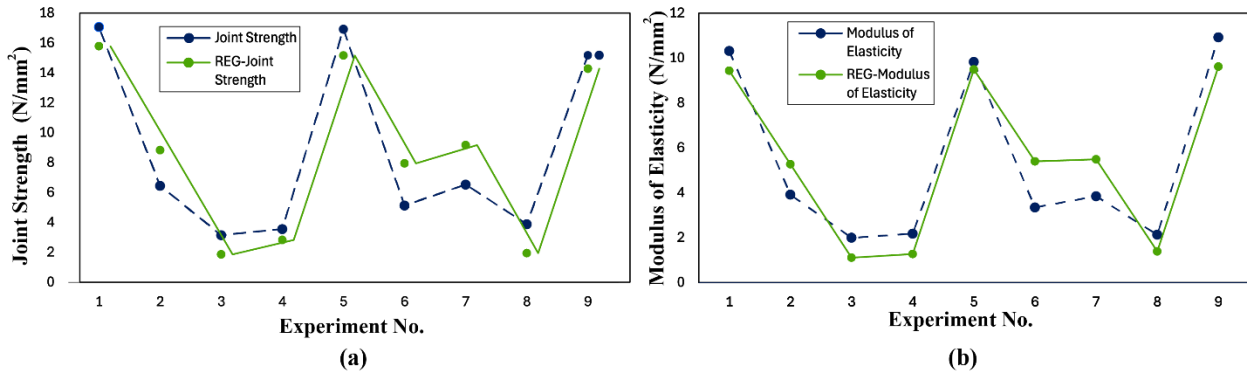


Figure 5. Comparing the predictions of regression models with experimental testing for (a) Joint strength (N/mm²) and (b) Modulus of Elasticity (N/mm²).

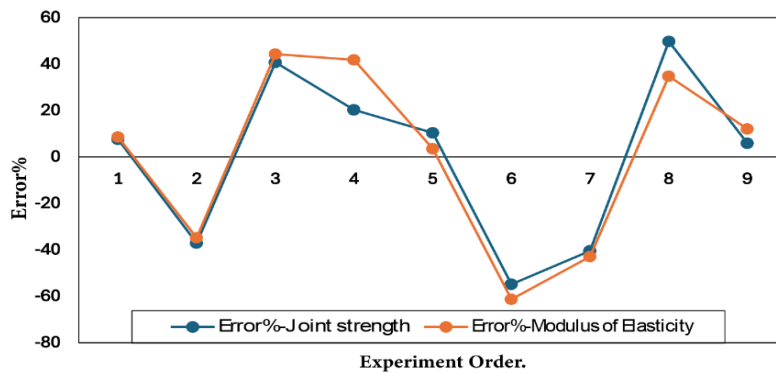


Figure 6. The error percentage of process responses.

4.4 Taguchi Quality Loss Function Approach

The results of normalized quality loss values, TNQL values, and MSNR values appear in **Table 5**. The goal is always to maximize the value of MSNR. The more MSNR value there is, the better the multi-quality features are. It has been shown that experiment one, among the nine experiments on welding, possesses the best multi-quality features in the current work, as it corresponds to the highest MSNR value, with parameter levels A1, B1, C1, and D1. The next step is to determine the average effect of each factor on the multiple quality characteristics at different levels, as shown in **Fig. 7**.

Table 5. Taguchi quality loss function method calculation

| Exp. No. | Weighted Normalized Quality Loss Value | | TNQL | MSNR (dB) | RANK |
|----------|--|-----------------------|----------|-----------|------|
| | Joint Strength | Modulus of Elasticity | | | |
| 1 | 0.020402 | 0.01490 | 0.01765 | 17.5320 | 1 |
| 2 | 0.143499 | 0.10370 | 0.122147 | 9.13114 | 4 |
| 3 | 0.6 | 0.4 | 0.5 | 3.0103 | 9 |
| 4 | 0.472827 | 0.33567 | 0.40425 | 3.93346 | 8 |
| 5 | 0.020764 | 0.01641 | 0.01858 | 17.3074 | 2 |
| 6 | 0.225767 | 0.14173 | 0.18374 | 7.35774 | 6 |
| 7 | 0.139634 | 0.10772 | 0.12367 | 9.07707 | 5 |
| 8 | 0.397074 | 0.34961 | 0.3733 | 4.27845 | 7 |
| 9 | 0.025803 | 0.01328 | 0.01954 | 17.0896 | 3 |



This is equivalent to the sum of all signal-to-noise ratios (S/N) corresponding to a factor at a certain level divided by the number of repetitions of that factor level. The delta specified in **Table 6** shows the MSNR variation for different welding parameters. It was found that the spot geometric size had the biggest impact on MSNR within the specified range of parameters. Therefore, spot geometric size is the most crucial parameter for quality, followed by welding velocity, laser power, and laser focus diameter.

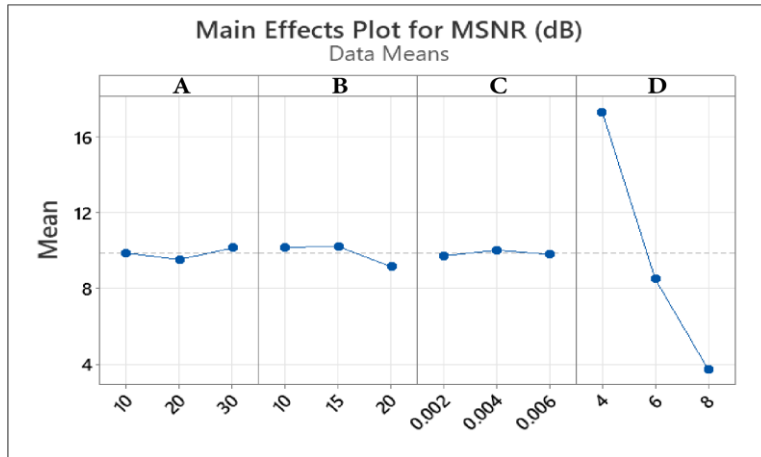


Figure 7. Main effects plot of welding parameters on MSNR

Table 6. Response table for means of MSNR

| Welding Parameters | Level 1 | Level 2 | Level 3 | Delta | Rank |
|-------------------------|---------|---------|---------|----------|------|
| Laser Power, A | 9.86 | 9.53287 | 10.1484 | 0.61553 | 3 |
| Welding Velocity, B | 10.1808 | 10.239 | 9.15255 | 1.08645 | 2 |
| Laser Focus Diameter, C | 9.72273 | 10.0514 | 9.79826 | 0.32867 | 4 |
| Spot Geometric Size, D | 17.3097 | 8.52198 | 3.74074 | 13.56896 | 1 |

4.5 TOPSIS Approach

The results of positive and negative separation values and proximity coefficient values are shown in **Table 7**.

Table 7. Calculation of TOPSIS method.

| Exp. No. | Weighted Normalized Responses | | Separation Positive | Separation Negative | Proximity Coefficient | RANK |
|----------|-------------------------------|-----------------------|---------------------|---------------------|-----------------------|------|
| | Joint Strength | Modulus of Elasticity | | | | |
| 1 | 0.331270 | 0.212570 | 0.01255 | 0.32003 | 0.9622637 | 1 |
| 2 | 0.124910 | 0.080577 | 0.25081 | 0.07615 | 0.2329115 | 4 |
| 3 | 0.061087 | 0.041029 | 0.32693 | 0 | 0 | 9 |
| 4 | 0.068813 | 0.044787 | 0.31843 | 0.00859 | 0.0262732 | 8 |
| 5 | 0.328372 | 0.202545 | 0.02276 | 0.31229 | 0.9320688 | 2 |
| 6 | 0.099584 | 0.068927 | 0.27941 | 0.04754 | 0.1454101 | 6 |
| 7 | 0.126627 | 0.079062 | 0.25141 | 0.07577 | 0.2315941 | 5 |
| 8 | 0.07509 | 0.043881 | 0.31380 | 0.01429 | 0.0435588 | 7 |
| 9 | 0.294569 | 0.225121 | 0.03670 | 0.29732 | 0.8901277 | 3 |



The aim is to maximize the proximity coefficient, as a higher value indicates better multi-quality features. The first experiment among nine experiments showed the best multi-quality features due to having the highest proximity coefficient value with parameters A1, B1, C1, and D1. The next step is to find the average effect of each factor on multiple quality characteristics at different levels by calculating the sum of proximity coefficient ratios for a factor at a certain level divided by the number of repetitions, as shown in **Fig. 8**. **Table 8** shows the delta for proximity coefficient variation for different welding parameters. It was found that the spot geometric size had the most significant impact on the proximity coefficient within the specified range of parameters. Therefore, spot geometric size is the most crucial parameter for quality, followed by welding velocity, laser power, and laser focus diameter.

Table 8. Response table for means of proximity coefficient.

| Welding Parameters | Level 1 | Level 2 | Level 3 | Delta | Rank |
|-------------------------|----------|----------|-----------|-----------|------|
| Laser Power, A | 0.398392 | 0.367917 | 0.388427 | 0.030475 | 3 |
| Welding Velocity, B | 0.40671 | 0.402846 | 0.345179 | 0.061531 | 2 |
| Laser Focus Diameter, C | 0.383744 | 0.383104 | 0.387888 | 0.004784 | 4 |
| Spot Geometric Size, D | 0.928153 | 0.203305 | 0.0232773 | 0.9048757 | 1 |

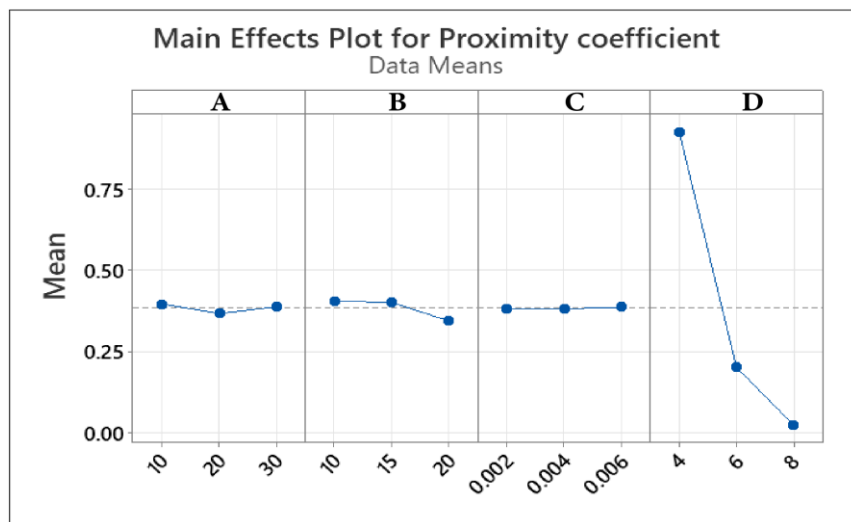


Figure 8. Main effects plot of welding parameters on the proximity coefficient

5. CONCLUSIONS

This research examined the mechanical properties of PMMA material samples welded using laser spot welding, like joint strength and modulus of elasticity. The welding parameters studied included laser power, welding velocity, laser focus diameter, and spot geometric size. A fiber laser with an orthogonal L9 array was used with four levels. (ANOVA) of the Regression (REG) model enhanced individual objectives. Multi-objective optimization techniques were used, as Taguchi Quality Loss Function, and the result was confirmed and compared using the TOPSIS method, selected criteria that matched all responses. The following results were obtained:

1. The percentage contribution from the REG model shows that spot geometric size has the most significant impact on joint strength at 87.90%. The other parameters, welding velocity, laser power, and laser focus diameter, contribute 0.80%, 0.08%, and 0.02%,



respectively. For elasticity modules, spot geometric size has the highest impact at 88.26%, laser power has a small impact at 0.07%, and welding velocity and focus diameter have no impact. The main effects plot showed decreased spot geometric size and laser power, with medium welding speed enhancing joint strength, regardless of laser focus diameter. Meanwhile, the modulus of elasticity increases with smaller spot size, higher laser power, and medium laser focus diameter, regardless of welding speed.

2. The result of the predicted model shows that the average error value in joint strength is 29.45%. Moreover, the average error value in modulus of elasticity is 31.54%. The observed errors are approaching an acceptable rate within the typical error range of the modeling tool.
3. After comparing the analysis of the TOPSIS method and the Taguchi Quality Loss Function method, it was found that their results were very similar. The first experiment among nine showed the best multi-quality features with parameters A1, B1, C1, and D1. The main effects plot showed that the spot geometric size significantly impacted the welding process at 4 mm in diameter. Therefore, spot geometric size is the most crucial parameter for quality, followed by welding velocity, laser power, and laser focus diameter.

NOMENCLATURE

| Symbol | Description | Symbol | Description |
|-----------|----------------------------|---------------|--|
| A | Laser Power | LSW | Laser Spot Welding |
| B | Welding Velocity | HAZ | Heat Affected Zone |
| C | Spot Geometric Size | ANOVA | Analysis of Variance |
| D | Laser Focus Diameter | Taguchi (QLF) | Taguchi Quality Loss Function |
| REG model | Regression Model | TOPSIS | Technique for Order Preference by Similarity to Ideal Solution |
| LTW | Laser Transmission Welding | PMMA | Polymethyl methacrylate |

Acknowledgements

The authors would like to express their sincere gratitude for support by the Department of Mechanical Engineering, College of Engineering, University of Baghdad.

Credit Authorship Contribution Statement

Ruba Khalil: Multi-Criteria Optimization of Mechanical Performance in Laser Spot Welding Process and writing the draft version. Bassim Bachy: development, follow-up, revision, and proofreading version.

Declaration of Competing Interest

The authors declare that they have no known competing financial interests or personal relationships that could have appeared to influence the work reported in this paper.

REFERENCES

Acherjee, B., 2020. Laser transmission welding of dissimilar plastics: Analyses of parametric effects and process optimization using grey-based Taguchi method. *Modern Manufacturing Processes*, May, pp. 131–144. <https://doi.org/10.1016/B978-0-12-819496-6.00006-3>



- Acherjee, B., 2020. Laser transmission welding of polymers–A review on process fundamentals, material attributes, weldability, and welding techniques. *Journal of Manufacturing Processes*, 60, pp.227-246.
- Acherjee, B., 2021. Laser transmission welding of polymers – A review on welding parameters, quality attributes, process monitoring, and applications. *Journal of Manufacturing Processes*, 64(April), pp. 421–443. <https://doi.org/10.1016/j.jmapro.2021.01.022>
- Alasfar, R. H., Ahzi, S., Barth, N., Kochkodan, V., Khraisheh, M., and Koç, M., 2022. A Review on the modeling of the elastic modulus and yield stress of polymers and polymer nanocomposites: Effect of temperature, loading rate and porosity. *Polymers*, 14(3). <https://doi.org/10.3390/polym14030360>
- AlMaadeed, M.A.A., Ponnamma, D. and Carignano, M.A. eds., 2020. *Polymer science and innovative applications: materials, techniques, and future developments*. Elsevier.
- Anwer, G., and Acherjee, B. 2024. Laser transmission welding of polypropylene: Insights into parameter interplay, thermal analysis, bonding quality, fracture characteristics, and weld morphology. *Journal of Materials Engineering and Performance*, 6. <https://doi.org/10.1007/s11665-024-09500-9>
- Bachy, B., and Franke, J. 2015. Experimental investigation and optimization for the effective parameters in the laser direct structuring process. *Journal of Laser Micro Nanoengineering*, 10(2), pp. 202–209. <https://doi.org/10.2961/jlmn.2015.02.0018>
- Bachy, B., Süß-Wolf, R., and Franke, J. 2018. On the quality and the accuracy of the laser direct structuring, experimental investigation and optimization. *Journal of Laser Applications*, 30(2), pp. 1–2. <https://doi.org/10.2351/1.5005629>
- Chokkalingam, P., El-Hassan, H., El-Dieb, A., and El-Mir, A. 2022. Multi-response optimization of ceramic waste geopolymer concrete using BWM and TOPSIS-based taguchi methods. *Journal of Materials Research and Technology*, 21(November), pp. 4824–4845. <https://doi.org/10.1016/j.jmrt.2022.11.089>.
- Dave, F., Mahmood Ali, M., Mokhtari, M., Sherlock, R., McIlhagger, A., and Tormey, D. 2022. Effect of laser processing parameters and carbon black on morphological and mechanical properties of welded polypropylene. *Optics and Laser Technology*, 153, pp. 108216. <https://doi.org/10.1016/j.optlastec.2022.108216>
- Dowling, N. E., 2013. *Mechanical behavior of materials: engineering methods for deformation, fracture, and fatigue*. Publisher Pearson. <https://books.google.iq/books?id=g1yCZwEACAAJ>
- Farabi, N., Chen, D. L., and Zhou, Y., 2012. Tensile properties and work hardening behavior of laser-welded dual-phase steel joints. *Journal of Materials Engineering and Performance*, 21(2), pp. 222–230. <https://doi.org/10.1007/s11665-011-9865-8>
- Forte, M. A., Silva, R. M., Tavares, C. J., and E Silva, R. F. 2021. Is poly(Methyl methacrylate) (PMMA) a suitable substrate for ALD?: A review. *Polymers*, 13(8). <https://doi.org/10.3390/polym13081346>
- Girish Kumar, R., Anand, B., Jabiulla, S., and Narasimha Murthy, H. N. 2023. Laser transmission welding (LTW) of three dimensional (3-D) printed polylactic acid (PLA) sheets. *Lasers in Engineering*, 54(4–6), pp. 295–311.
- Girish Kumar, R., Narasimha Murthy, H. N., Anand, B., and Jabiulla, S. 2021. Parametric study of laser welding on polyamide using design of experiments. *Journal of Physics: Conference Series*, 1950(1). <https://doi.org/10.1088/1742-6596/1950/1/012042>



- Haqi, I. A., and Olfat A. M., 2021. The study of the effect of zirconium oxide nanoparticles (zro 2) and multiwall carbon nanotubes (mwcnts) on some mechanical properties of pmma nanocomposites. *Design Engineering*, pp. 5911–5936. <https://doi.org/10.13140/RG.2.2.27817.57441>
- Hassan, S. S., and Bachy, B. S., 2023. On the laser micro cutting: Experimentation and mathematical modeling based on RSM-CCD. *Journal of Engineering*, 29(6), pp. 98–113. <https://doi.org/10.31026/j.eng.2023.06.08>
- Huang, Y., Gao, X., Ma, B., and Zhang, Y. 2021. Interface formation and bonding mechanisms of laser welding of PMMA plastic and 304 austenitic stainless steel. *Metals*, 11(9). <https://doi.org/10.3390/met11091495>
- Hussein, S. A., and Bachy, B. S., 2024. Evaluation of joint strength in laser transmission welding of PMMA polymer. *Association of Arab Universities Journal of Engineering Sciences*, 31, pp. 13–23.
- Ilie, M., Stoica, V., Cicala, E., and Kneip, J. C. 2020. Experimental design investigation of through-transmission laser welding of dissimilar polymers. *Journal of Physics: Conference Series*, 1426(1). <https://doi.org/10.1088/1742-6596/1426/1/012045>
- Imran, H. J., Hubeatir, K. A., and Al-Khafaji, M. M. 2021. CO2 laser micro-engraving of PMMA complemented by Taguchi and ANOVA methods. *Journal of Physics: Conference Series*, 1795(1). <https://doi.org/10.1088/1742-6596/1795/1/012062>
- Jiang, X., Chandrasekar, S., and Wang, C., 2015. A laser microwelding method for assembly of polymer based microfluidic devices. *Optics and Lasers in Engineering*, 66, pp. 98–104.
- Judawisastra, H., Claudia, Sasmita, F., and Agung, T. P. 2019. Elastic modulus determination of thermoplastic polymers with pulse-echo method ultrasonic testing. *IOP Conference Series: Materials Science and Engineering*, 547(1). <https://doi.org/10.1088/1757-899X/547/1/012047>
- Kanaujia, N., Rahul, Behera, J. K., Kumar Mohapatra, S., Behera, A., Jha, P., Kishore Joshi, K., and Chandra Routara, B. 2022. Process parameters optimization in CNC turning of aluminum 7075 alloy using TOPSIS method coupled with Taguchi philosophy. *Materials Today: Proceedings*, 56(July), pp. 989–994. <https://doi.org/10.1016/j.matpr.2022.03.226.zzz>
- Khalaf, B.A. and Kadhim, B.S., 2023. Use of the quality loss function for improving the productive processes in the general company for the automotive industry–Alexandria–An applied research. *International Journal of Innovation, Creativity and Change*, 14(7), p.p 148-165.
- Kucukoglu, A., Yuce, C., Sozer, I. E., and Karpaz, F. 2023. Multi-response optimization for laser transmission welding of PMMA to ABS using Taguchi-based TOPSIS method. *Advances in Mechanical Engineering*, 15(8), pp. 1–16. <https://doi.org/10.1177/16878132231193260>
- Kumar Goyal, D., Yadav, R., and Kant, R. 2023. Laser transmission welding of polycarbonate sheets using electrolytic iron powder absorber. *Optics and Laser Technology*, 161(January), P.109165. <https://doi.org/10.1016/j.optlastec.2023.109165>
- Li, Q., Mu, Z., Luo, M., Huang, A., and Pang, S. 2021. Laser spot micro-welding of ultra-thin steel sheet. *Micromachines*, 12(3). <https://doi.org/10.3390/mi12030342>
- Milislavljevic-Syed, J., Petrovic, E., Ćirić, I., Mančić, M., Milislavljević, J., Petrović, E., Marković, D., and Đorđević, M. 2012. *the Danubia-Adria Symposium*. 29 May 2014. <https://www.researchgate.net/publication/256096156>



- Olowinsky, A., and Roesner, A. 2012. Laser welding of polymers established process but still not at its best the authors. *Laser Technik Journal*, April (2), pp. 52–56.
- Rane, S.S., Srividya, A. and Verma, A.K., 2011. Use of Taguchi loss function in deformation based multi-response optimization of motorcycle frame. *Communications in Dependability and Quality Management*, 14(4), pp. 19-31.
- Röhrich, M. L., Stichel, T., Roth, S., Bräuer, P. A. B., Schmidt, M., and Will, S. 2020. Correlation between weld seam morphology and mechanical properties in laser transmission welding of polypropylene. *Procedia CIRP*, 94(March), pp. 691–696. <https://doi.org/10.1016/j.procir.2020.09.119>
- Rudrapati, R., Kumar, N., and Pal, P. K. 2019. Application of Taguchi method for parametric optimization of through transmission laser welding of acrylic plastics. *AIP Conference Proceedings*, 2057(January). <https://doi.org/10.1063/1.5085584>
- Sabry, I., Hewidy, A. M., Naseri, M., and Mourad, A. H. I. 2024. Optimization of process parameters of metal inert gas welding process on aluminum alloy 6063 pipes using Taguchi-TOPSIS approach. *Journal of Alloys and Metallurgical Systems*, 7(June), P. 100085. <https://doi.org/10.1016/j.jalms.2024.100085>
- Schkutow, A., and Frick, T. 2016. Influence of adapted wavelengths on temperature fields and melt pool geometry in laser transmission welding. *Physics Procedia*, 83, pp. 1055–1063. <https://doi.org/10.1016/j.phpro.2016.08.111>
- Shaker, F., AL-Khafaji, M., and Hubeatir, K. 2020. Effect of different laser welding parameter on welding strength in polymer transmission welding using semiconductor. *Engineering and Technology Journal*, 38(5), pp. 761–768. <https://doi.org/10.30684/etj.v38i5a.368>
- Sharma, A., Awasthi, A., Singh, T., Kumar, R., and Chauhan, R. 2022. Experimental investigation and optimization of potential parameters of discrete V down baffled solar thermal collector using hybrid Taguchi-TOPSIS method. *Applied Thermal Engineering*, 209 (September 2021), P. 118250. <https://doi.org/10.1016/j.applthermaleng.2022.118250>
- Sultana, N., and Dhar, N. R. 2021. Hybrid GRA-PCA and modified weighted TOPSIS coupled with Taguchi for multi-response process parameter optimization in turning AISI 1040 steel. *Archive of Mechanical Engineering*, 68(1), pp. 23–49. <https://doi.org/10.24425/ame.2020.131707>
- Tshibangu, W. M. A. 2018. Taguchi loss function to minimize variance and optimize a flexible manufacturing system (FMS): A six sigma approach framework. *ICINCO 2018 - Proceedings of the 15th International Conference on Informatics in Control, Automation and Robotics*, 2, pp. 592–599. <https://doi.org/10.5220/0006868705920599>
- Umamaheswarrao, P., 2023. Multi-response optimization of process parameters during friction stir welding of AA2014-AA7075 using TOPSIS Approach. *Incas Bulletin*, 15(1), pp. 107–117. <https://doi.org/10.13111/2066-8201.2023.15.1.10>
- Van Pham, D. 2023. Research to determine the best value of both Z and Ovc in micro-edm using carbon coated electrode using TOPSIS method. *EUREKA, Physics and Engineering*, 2023(3), pp. 90–96. <https://doi.org/10.21303/2461-4262.2023.002790>

TOPSIS مقابل دالة فقدان الجودة لتحسين الأداء الميكانيكي متعدد المعايير في عملية

اللحام بالليزر النقطي

ربى خليل *، باسم باشي

قسم الهندسة الميكانيكية، كلية الهندسة، جامعة بغداد، بغداد، العراق

الخلاصة

عند اختيار مادة لتصميم المنتج ينصب التركيز على خصائصها الميكانيكية، حيث أن هذا يتطلب قياسي في معظم التطبيقات. هدف هذا البحث هو تحديد ما إذا كان من الممكن تحقيق معايير أفضل لعينات مادة بولي ميثيل ميثاكريلات الملحومة بلحام الليزر النقطي من خلال التحقق من أداء قوة المفصل ومعامل المرونة. أجريت اختبارات الشد باستخدام آلة اختبار عالمية بسعة تحميل 100 كيلو نيوتن. وشملت المعلمات المدروسة قوة الليزر، سرعة اللحام، قطر بؤرة الليزر، وحجم القطر الهندسي. تم استخدام مصفوفة L9 متعامدة بثلاث مستويات. وتم استخدام تقنيات التحسين متعددة الأهداف - TOPSIS - دالة فقدان الجودة، وتم مقارنة النتائج. وقد اكتشف أن التجربة الأولى من بين التجارب التسع لها أفضل ميزات متعددة الجودة مع معلمات طاقة الليزر عند (10) واط، سرعة اللحام عند (10) ملم/ثانية، قطر بؤرة الليزر عند (0.002) ملم، وحجم القطر الهندسي عند (4) ملم. وقد لوحظ أن تصميم القطر الهندسي هو المعلمة الأكثر تأثيراً على الجودة عند الحجم الصغير، وهذا يثبت أن الحجم الأصغر يزيد من قوة وصلابة المنتج الملحوم.

الكلمات المفتاحية: عملية لحام بالليزر النقطي، الخواص الميكانيكية، اختبار الشد، قوة المفصل، معامل المرونة، مادة البولي ميثيل ميثاكريلات.